A Soft Robotic Glove Providing Proprioceptive Feedback for Grip Force Regulation Training

Yixing Lei[1], Ryman Hashem[1], Mauricio Villarroel[1], and Liang He[1]

Abstract— Inadequate regulation of grip force during tennis strokes may contribute to wrist and elbow overuse injuries. Although force transducer technologies such as strain gauge and piezoelectric sensors can quantify grip force, training feedback has largely been limited to visual feedback. The potential benefit of proprioceptive haptic feedback in grip force regulation training remains unclear.This study presents a soft robotic training system integrating a strain gauge embedded in a tennis racket for grip force sensing and an pneumatic actuator that provides proprioceptive haptic feedback. A pilot study was conducted in one novice tennis player to evaluate system feasibility and demonstrate its functionality. A passive force regulation experiment first verified the actuator's ability to deliver physical haptic guidance. Then, during the active force regulation training, differences in learning curve and retention were observed between visual and haptic feedback conditions. Learning improvement, quantified as error reduction from pre- to post-training, reached 39% of the target force under visual feedback and 37% under haptic feedback. In retention trials, the root mean square error (RMSE) was 23.6% following visual feedback training and 20.0% following haptic feedback training. These preliminary findings suggest potential differences in training efficiency between feedback modalities. Further studies with larger samples are required to determine the generalizability of these observations and to further evaluate the effectiveness of the proposed soft robotic training system.

I. Introduction

Tennis elbow is a common and serious concern among tennis players. Repetitive exposure to high forces and unnatural arm positions during strokes subjects the muscles and tendons to excessive torque, often resulting in wrist and elbow injuries such as tendinopathy and lateral epicondyles [1]. A study of 568 tennis players in a tennis club aged 20–50 in the northeastern United States found that 39.7% had been affected by tennis elbow, including 75 current (incident or recurrent) cases and 136 with a prior history [2]. Among the key risk factors, inadequate grip force is one of the most prevalent. During play, a tight grip stiffens the wrist, reducing its ability to absorb shock and adapt to stroke variations, which can lead to micro-trauma at the tendon origin of the extensor muscle group[3]. The risk becomes greater during off-center impacts below the racket's longitudinal axis, where excessive grip pressure produces high eccentric wrist extension torques and forced wrist flexion [4]. Conversely, an overly loose grip compromises racket stability, which may induce wrist tendinopathy and reduce overall performance. Simulations have suggested that wrist flexion and low muscle activation during ball impact could contribute to repetitive micro-trauma and lead to injury as well[5]. Although studies have been done in measuring grip pressure during tennis playing, approaches that deliver feedback to players remain unexplored. Recent sensing technologies such as pressure mat [6], piezoresistive pressure sensors [7] have been directly used with tennis racket for pressure measuring. Strain gauges have been used in grip force measuring within a handler [8]. For feedback providing, the motor training experiment regarding to grip force regulation are mainly use the method that visualizing the error as external cues for motor control [9], [10]. However, motor learning theory emphasizes that skill acquisition hinges on the formation of internal models that link sensory feedback to motor commands[11]. If training relies too heavily on external information (e.g. constant visual displays), performance can degrade once those cues are withdrawn, and novices may experience cognitive overload [12]. Consequently, it is important to understand whether haptic feedback that supports force regulation training while preserving natural sensorimotor integration.

Despite advances in haptics feedback device, there is a gap in conveying force-magnitude information thorugh haptic feedback. Many wearable and robotic systems provide spatial or temporal cues via vibration or pressure based actuators. However, these signals do not replicate the proprioceptive/ kinaesthetic information people use to modulate continuous grip force. To address this, we propose using a soft-robotic glove that delivers proprioceptive haptic feedback. Robotic gloves have been increasingly employed in motor learning and rehabilitation. Various designs, including rigid exoskeletons [13], [14], robotic actuation systems [15], [16], and pneumatic gloves [17], have been developed to facilitate the training of fine motor skills such as dexterity and pinch-force control. Exoskeleton-based systems primarily target joint kinematics but often face challenges related to fit, alignment, and user comfort. In contrast, soft pneumatic gloves have been extensively investigated for rehabilitation applications, such as providing passive repetitive assistance or facilitating mirror therapy. Nevertheless, even when force sensors are included [17], these systems are typically compensatory rather than designed for active force-regulation training.

*This work was supported by the Podium Institute for Sports Medicine and Technology.

[1]The Institute of Biomedical Engineering, Department of Engineering Science, University of Oxford. yixing.lei@eng.ox.ac.uk

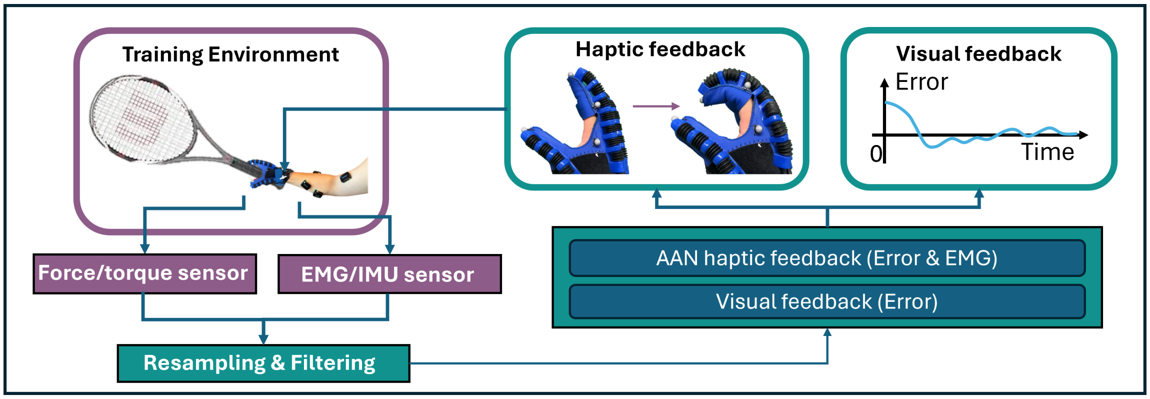

Fig. 1: Overall design of system and dataflow. Force and torque signal on the racket and surface Electromyography (EMG) and inertial measurement unit(IMU) signals were acquired and synchronized. All data streams were collected and resampled, and synchronized with a fixed delay of 30 ms to enable real-time processing. The resampled data were then processed according to the desired feedback mode, generating control commands. These output signals were transmitted to both the soft robotic glove and graogical user interface (GUI) to provide haptic and visual feedback, respectively

In our system, a six-axis load cell was embedded in the racket grip measures net grip forces and moments. We calibrate the measurement with EMG signal from extensor and flexor muscle groups. A pneumatic glove delivers haptic feedback to support active training of grip-force regulation with an EMG-informed assist-as-need (AAN) control mechanism. This work is aimed to introduce this visual-haptic soft robotics training system with all sensor and device calibration and characteristic. A piolet study was conducted to demonstrate the functional capability of the proposed system.

II. Design and calibration of the training system

We developed a tennis racket grip training system designed to deliver haptic feedback conveying grip-force magnitude during force regulation tasks. The overall system architecture is illustrated in Fig. 1. A six-axis force/torque sensor was integrated into the racket handle and sampled at 2000 Hz to measure grip-generated forces and torques. Data were acquired using a USB-6451 data acquisition device (National Instruments, USA). This configuration enables high–temporal-resolution force profiling and allows vibration signals to be captured for subsequent analysis. Two Delsys Trigno sensors, equipped with EMG and IMU modes, were positioned over the Extensor Carpi Radialis Brevis (ECRB) and Flexor Carpi Radialis (FCR) to record muscle activity and local kinematics at 1259 Hz. Data were streamed via the Delsys API using Python. All signals were resampled to 1200 Hz for synchronization. A fixed 30 ms delay was introduced to ensure stable real-time processing. The processed signals were fed into a feedback algorithm, whose output updated both the soft robotic glove (haptic feedback) and the visual interface at a rate of 20 Hz.

Fig. 2 illustrates the sensor implementation and the pneumatic control system used in the proposed setup. The force/torque sensor (Schunk SI 125-3, Schunk, Germany) is embedded inside the grip and mounted to measure both the normal pressure force and the torque generated during twisting motions shown as Fig. 2(A,B). Surface EMG sensors (Delsys, USA) are placed on the forearm over the extensor and flexor muscle groups to monitor muscle activity related to grip force generation. The sensor placement is shown in Fig. 2(C), where one sensor detects activity in the extensor group and the other in the flexor group, the two primary muscle groups responsible for grip control. Haptic feedback is provided through the pneumatic glove (Yisheng, China) showed in Fig. 2(D), where the chamber pressure for each finger can be controlled within a range of −100 kPa to 200 kPa. The pneumatic control of the glove is achieved using a pressure regulation system that enables precise and stable control. During tennis play, various grip styles are used depending on player preference and technical requirements, which may result in different load cell responses. Thus, we compared the effect for force detecting using western grip styles and continental grip style shown as Fig. 2(E). In continental grip style, the thenar web space of the player would face 5th bevel of the grip and have index finger on bevel 6 and 7 where the force could mainly come from the flexing of index finger and thumb. When performing the western grip, the thenar web space of player would face bevel 7. Fig. 2(F) shows the setup during training.

A. Calibration and characteristic

1) Characteristic of EMG: The objective of this calibration process was to establish a regression model for predicting voluntary grip force from EMG signals. To this end, a force–torque sensor was integrated into the racket grip, and the performance of the embedded sensing system was characterized. Sensor measurements were compared with EMG recordings to evaluate the validity of the system and to determine the relationship between muscle activation and grip force. Accordingly, a

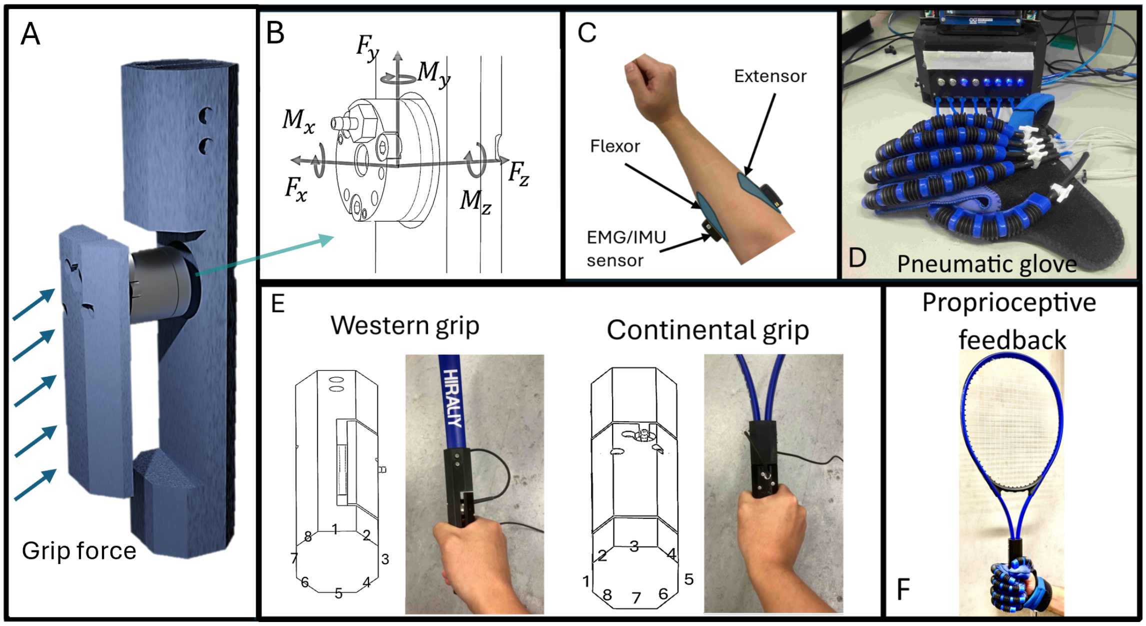

Fig. 2: Devices included in the training system. (A, B) A six-axis force/torque sensor (Schunk SI 125-3, Schunk, Germany) is embedded inside a 3D-printed tennis grip, with the measuring head connected to a pad contacting only the sensor surface. (C) Surface EMG sensors (Delsys, USA) are attached to both sides of the forearm, targeting the flexor and extensor muscle groups (illustrated in blue). (D) A pneumatic glove provides haptic feedback and is connected to a pressure regulator (VEAB-B, Festo, Germany). (E) The two grip styles. (F) Participant with assistant glove.

calibration procedure and EMG signal analysis were conducted. Participant first performed maximum voluntary contractions (MVCs) of the wrist flexor and extensor muscles separately, with three repetitions for each muscle group. EMG signals were recorded during these trials and subsequently processed to obtain root mean square (RMS) values using the following equation:

$$\text{RMS}\{x\} = \sqrt{\text{MA}_T(|\text{BP}\{x\}|^2)} \tag{1}$$

where MA_T represents the mean average over the time period T, and BP denotes the bandpass filter (20–450 Hz) applied by the Delsys sensor. The RMS values obtained during the MVC periods were averaged and saved as $MVC_{extensor}$ and MVC_{flexor}, respectively. For each participant, the RMS values during the experiment were normalized using these reference values and expressed as a percentage of MVC (%MVC).

A regression analysis was conducted using RMS_{max} to estimate the force that generated. The equation for the regression is set as:

$$F_{estimate} = a * RMS_{flexor} + b * CCI + c \tag{2}$$

The flexor muscle group is primarily responsible for generating force during a power grip, whereas the extensor muscle group contributes mainly to stabilization [18]. The co-contraction index (CCI), where c denotes a constant, quantifies the simultaneous activation of agonist and antagonist muscle pairs. Increased co-contraction enhances joint stiffness without necessarily increasing the net output force, as both muscle groups exhibit elevated activity. The CCI is calculated using the equation proposed by Falconer and Winter [19]:

$$CCI = \frac{2 * RMS_{low}}{RMS_{low} + RMS_{high}} \tag{3}$$

A least square optimization is used to calculate coefficient a, b and c. With regression model the RMS trail have been used to predict the force generated in the whole trail. The regression RMSE is 22.24 with R2 equals to 0.89.

2) Characteristic of force torque sensor: The aim of this experiment is to evaluate the correlation between EMG data and force measurement from the grip. To investigate the relationship between force output and muscle activity, a comparative analysis was performed across different grip styles. Each participant was instructed to produce target resultant force magnitudes ($|F|$) of 60 N and 100 N, as well as to perform trials involving transitions from a relaxed state to a maximal power grip. The corresponding force profiles are shown in Fig. 3. The blue line represents the target normal force ($|F|$), and the orange line denotes the resultant moment magnitude ($|M|$). The upper panels of each trial illustrate the RMS variations in muscle activity, which generally correspond to changes in force output. The average directions of the resultant force and moment vectors across trials are summarized in Table I.

From Fig. 3, it can be observed that achieving the target $|F|$ values required moments of comparable magnitude across grip styles. During the 60 N target trials, the average torque was 1.8 Nm for the continental grip and 1.5 Nm for the western grip. When the target force

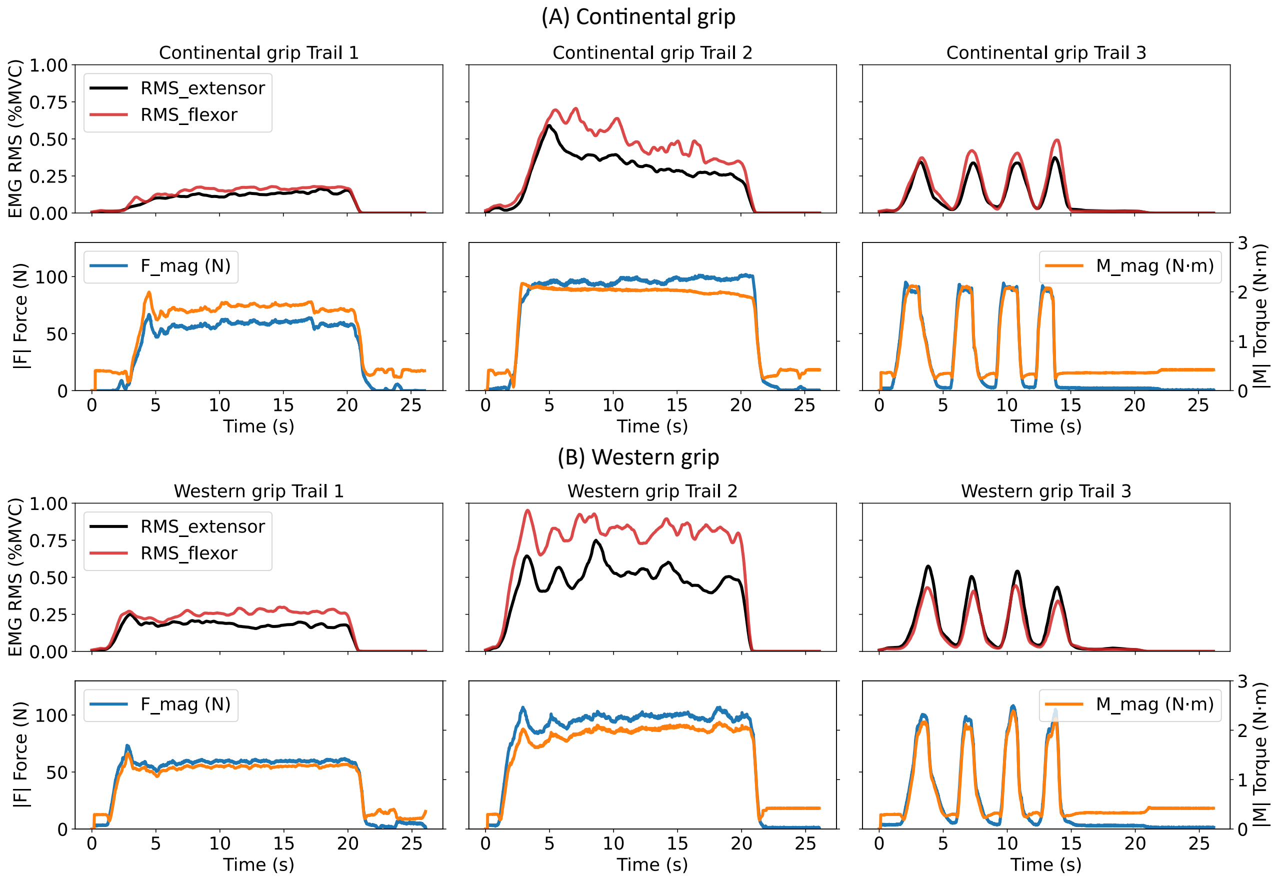

Fig. 3: Comparison between continental (A) and western (B) grip styles. In Trials 1 and 2, participants were instructed to regulate the resultant force magnitude ($|F|$) to 60 N and 100 N under visual guidance. The blue line represents the measured force output, while the orange line indicates the corresponding moment generated during the task. In Trial 3, participants repetitively varied their grip from minimal to maximal force.

TABLE I: Direction vectors of force (F) and moment (M) for two grip styles under 60 N and 100 N load conditions.

Condition	Force (F)			Moment (M)		
	x	y	z	x	y	z
Continental						
60N	0.07	−0.28	−0.93	0.54	0.00	0.44
100N	0.08	−0.35	−0.92	0.55	0.10	0.41
Western						
60N	−0.07	−0.28	−0.95	0.60	0.24	0.28
100N	−0.01	−0.33	−0.93	0.50	0.30	0.25

increased to 100 N, the average peak torque for both grip styles was approximately 2 Nm. Across all trials, the averaged torque produced in continental grip remained higher than that of the western grip. Additionally, EMG data indicated greater flexor muscle activation when using the western grip compared to the continental grip, suggesting higher muscular effort associated with this configuration. As shown in Table I, the magnitude of $|F|$ was similar for both grip types, but the torque vector $|M|$ exhibited a major difference in direction between the two grips.

3) Characteristic of pneumatic glove: Before the regulation task, it's necessary to estimate the force enerate by the glove given different pressure in the chamber. Building upon the previous calibration results, the relationship between EMG activity and the measured force and torque was clearly established. In this section, we evaluate how variations in glove chamber pressure influence the corresponding force sensor readings. The calibration was conducted under two grip conditions: a relaxed grip and a tight grip. During both procedures, the pressure within the glove chambers was cyclically varied between −100 kPa and 200 kPa, as illustrated in the pressure–force diagram in Fig.4.

In the relaxed-grip calibration Fig.4(A), when the chamber pressure was below 0 kPa, the hand was extended and did not contact the handle, resulting in no measurable force output. Once the pressure exceeded 0 kPa, a distinct increase in grip force was observed, while no substantial change in RMS muscle activity was detected. The average maximum force recorded under this relaxed condition was 15 N. The coefficient describing the relationship between chamber pressure and force generation during this phase was determined

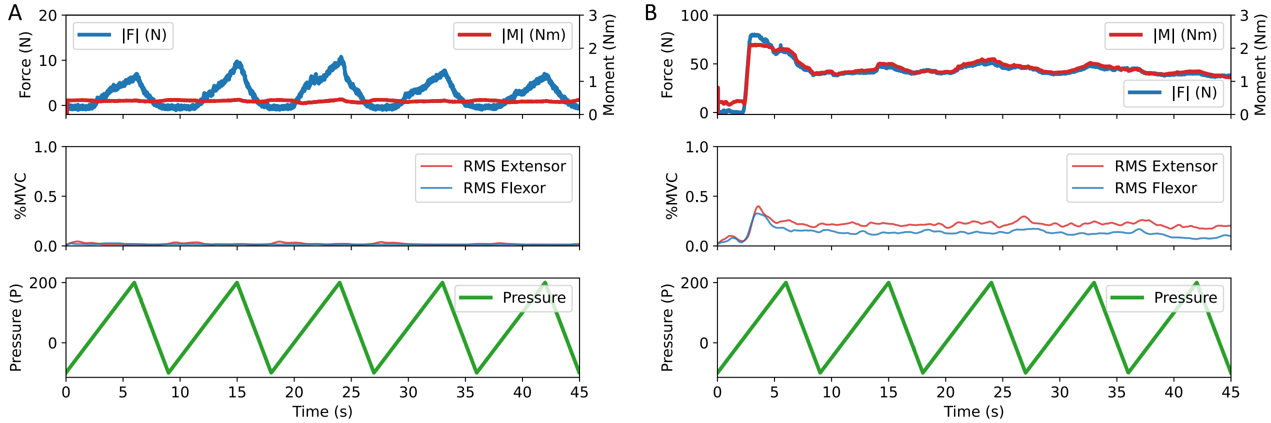

Fig. 4: Calibration of the pressure–force coefficient. (A) Participants maintained a relaxed grip while wearing the pneumatic glove. The top panel shows the force and torque variations detected by the sensor, the middle panel illustrates muscle activity that remaining near zero during relaxation. The bottom panel displays the cyclic pressure changes. (B) Participants performed a tight grip while the glove pressure was repeatedly varied between –100 kPa and 200 kPa. The middle panel indicates increased muscle activation corresponding to the pressure modulation

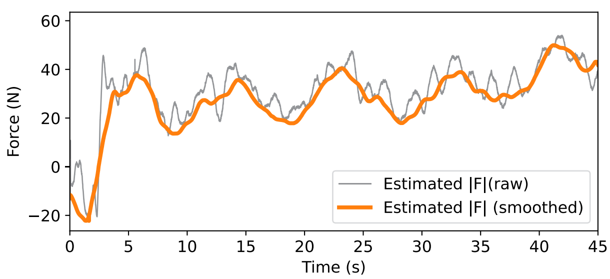

Fig. 5: Illustration of the difference between EMG-predicted force and measured force during cyclic pressure changes in the glove. Under the tight-grip condition, a regression model was applied to estimate voluntary force output from EMG signals, enabling separation of force variations induced by voluntary motion from those caused by glove pressure fluctuations.

as $C_{increase} = 0.075,\ F = P * C_{increase}, 200 > P > 0$.

In tight grip condition, the force $|F|$ change, pressure change and RMS change is shown in Fig.4(B). However, when voluntary contraction is conducted, it's difficult to distinguish the force change generate by glove and the force change caused by muscle control vibration. The regression model built in last section is used to estimate the force that generate with muscle, with the subtraction is the estimated force change caused by pressure change of pneumatic glove shown as Fig. 5. The decrease of force is calculated with following equation with $C_{decrease} = 0.10,\ F = P * C_{decrease}, 0 > P > -100$.

B. Feedback Design

Both visual and haptic feedback were employed in this study to guide participants during the training tasks. To provide intuitive feedback based on the collected sensor data, the following representation methods and control functions were implemented. Force feedback was visualised as a real-time line graph displayed using python plotting GUI with a refresh rate of 20 Hz. The target (desired) force was represented by a stationary horizontal line, while the measured force was plotted dynamically in real time, allowing participants to continuously monitor their grip performance. A tolerance band of ±2.5% around the target force was also displayed to indicate the acceptable range of force error. The haptic guidance followed an AAN principle, providing corrective feedback only when the participant's performance deviated from the target. The direction of the feedback force was set opposite to the error direction, in contrast to error-augmentation methods that amplify deviations. The desired feedback force was determined using both the force error and the rate of change of the EMG signal, which reflects the participant's voluntary muscle activity. The base control law for the feedback force was defined as:

$$F_{d_{\text{error}}} = -K(e)e - B\frac{de}{dt}, \tag{4}$$

where $K(e)$ is the stiffness gain and B is the damping coefficient. An adaptive modulation factor $\gamma \in [0, 1]$ was introduced to scale the feedback according to voluntary EMG activity:

$$F_d = \gamma \times F_{d_{\text{error}}}, \tag{5}$$

where γ reflects whether the EMG change corresponds to a corrective (appropriate) or erroneous (opposite) effort. This adaptive scaling allows the system to reduce haptic assistance when the participant is voluntarily correcting the error, thereby promoting motor learning. A guidance-free zone of ±2.5% around the target force was implemented to ensure that participants could still perform voluntary corrections without continuous haptic intervention.

III. Pilot study

A pilot study was conducted to demonstrate the capability of the training system in providing physical guidance and to compare the training efficiency of the two feedback modalities. The first part of the pilot study involved a passive force regulation experiment, in which a target force was predefined and the participant was instructed to modulate their grip accordingly. The task consisted of three stages: (1) relaxation with the control system deactivated, (2) relaxation with the control system activated, and (3) active contraction with the control system activated. The assistive force range of the pneumatic glove was between –10 N and 15 N; therefore, the target force was set at 10 N. Three repetitions were performed to evaluate performance. The second part of the pilot study involved force regulation training under different feedback conditions and was divided into training and retention phases. Six training trials were included in the training phase, with 1 minute of rest between trials. Each trial consisted of a 10 s non-feedback baseline stage, a 15 s feedback training stage, and a 10 s non-feedback post-training stage. A 10 s rest period was provided between stages. During each training trial, the participant held the racket with wrist support and adjusted their grip force. Haptic or visual cues were provided only during the feedback training stage to indicate the target force. Feedback was triggered when the force error exceeded 2.5% of the target force. After six training trials, the participant rested for 2 minutes before entering the retention phase. During the retention phase, three 10 s performance trials were completed, in which only terminal feedback was provided, with 10 s of rest between trials. After the retention phase, the target force was randomly changed to a new value between 20 and 100 N for the next training session.

A. Result

An example result of the passive force regulation trails are presented in Fig. 6. The averaged RMSE after control on is 3.34 when participant was relax and 7.60 when participants actively grasp. The limited force range of the glove restrict it's capability in fully control the grip force, however, it shouldn't affect it's capability in using as a guidance tool.

The outcomes of the force regulation training with haptic feedback are shown in Fig. 7. In this trial, the target force was set to 40 N. The root mean square error (RMSE) during the baseline, training, and non-feedback trials was analysed, yielding an overall average error of 20% of the target force. The mean reduction in RMSE from baseline to training trials was 36.6% of the target force, while the reduction between training and non-feedback trials was 3% of the target force. During the retention trials, the mean RMSE was 20% of the target force.

The results of the force regulation training with visual feedback are presented in Fig. 8. In this trial, the target force was set to 50 N. The overall average error across all trials was 19.9% of target force. The mean reduction in RMSE from baseline to training trials was 39% of the target force., which was greater than that observed in the haptic feedback group. The reduction between training and non-feedback trials averaged 4.3% of the target force, while the mean RMSE during retention trials was 23.6% of the target force .

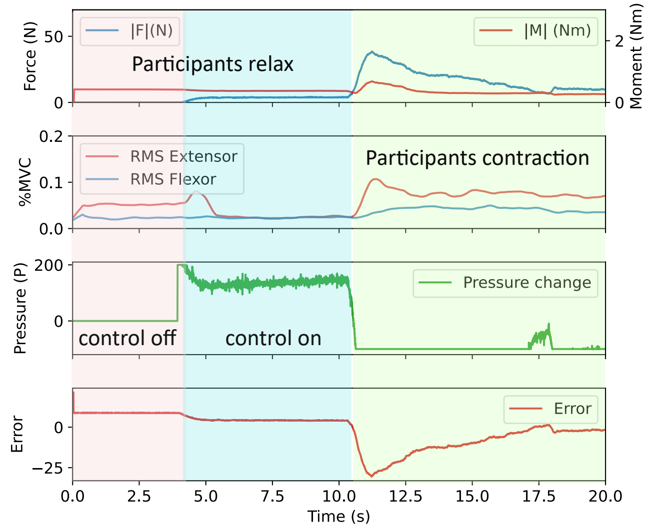

Fig. 6: Force regulation task with glove assistance. Participants remained relaxed during the pink and blue phases, and performed contractions during the green phase. The control was off in the pink phase and active in both the blue and green phases. The top panel illustrates changes in the resultant force magnitude ($|F|$) measured by the force/torque sensor during the glove-assisted regulation task. The second panel shows corresponding muscle activity. The third panel presents the chamber pressure profile. An overshoot near the end of the trial corresponds with the trend observed in the error data shown in the bottom panel.

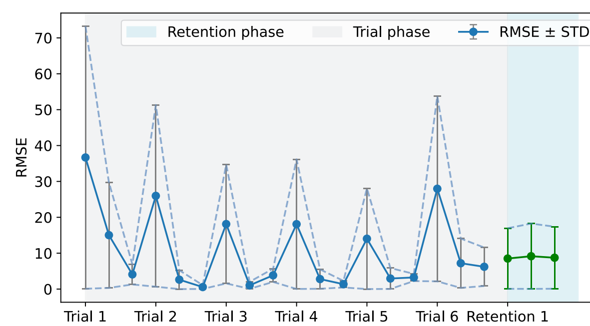

Fig. 7: Training and retention results from the force regulation experiment with haptic feedback. Each trial consisted of baseline, training, and non-feedback sessions. Performance across trials was quantified using RMSE, with standard deviations indicated. Retention tests were performed after the training phase without feedback.

The findings of this study demonstrate the feasibility of using a soft robotic glove as a haptic feedback modality for force regulation training. In particular, the retention outcomes from both visual and haptic feedback conditions support the initial hypothesis: visual feedback facilitates faster learning, whereas haptic feedback yields superior retention. These preliminary results lay the

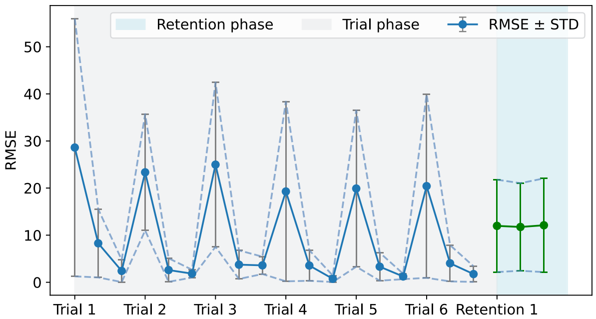

Fig. 8: Training and retention results from the force regulation experiment with visual feedback. Each trial included baseline, training, and non-feedback phases. Retention tests were conducted after training without feedback.

groundwork for future large-scale studies involving multiple participants to further evaluate learning efficiency and long-term retention in force regulation training.

IV. Conclusion

This study demonstrates the feasibility of using a haptic–visual feedback system in motor learning research. By varying feedback across modalities, we examined how differences in error representation influence the learning process. Although this study primarily focused on behavioural outcomes, the collected EMG data provide valuable opportunities for future investigations into motor command modelling and for exploring how different error presentations affect sensorimotor processing in the brain. As a pilot study, the number of participants was limited, and the generalizability of the findings needs to be validated in larger-scale studies. In addition, the experimental task involved static grip force regulation, which differs from real-world dynamic grip control. The underlying mechanisms and the extent to which static force regulation training transfers to dynamic tasks remain unclear and warrant further investigation. Nevertheless, the results support the feasibility of the system and the potential of the proposed hypotheses. Future research with a larger cohort is recommended to further validate and extend these findings.

ACKNOWLEDGMENT

The authors thank Jiayu Tang and Ria Prakash for their helpful and fruitful discussions. Funding: This work was supported by The Podium Institute for Sports Medicine and Technology, University of Oxford.

References

[1] H. Patel, S. Lala, B. Helfner, and T. T. Wong, “Tennis overuse injuries in the upper extremity,” Skeletal radiology, vol. 50, no. 4, pp. 629–644, 2021.

[2] H. W. Gruchow and D. Pelletier, “An epidemiologic study of tennis elbow: Incidence, recurrence, and effectiveness of prevention strategies,” The American Journal of Sports Medicine, vol. 7, no. 4, pp. 234–238, 1979, pMID: 474862. [Online]. Available: https://doi.org/10.1177/036354657900700405

[3] C. J. Rigozzi, G. A. Vio, and P. Poronnik, “Comparison of grip strength, forearm muscle activity, and shock transmission between the forehand stroke technique of experienced and recreational tennis players using a novel wearable device,” Sensors, vol. 23, no. 11, p. 5146, 2023.

[4] M. A. King, B. B. Kentel, and S. R. Mitchell, “The effects of ball impact location and grip tightness on the arm, racquet and ball for one-handed tennis backhand groundstrokes,” Journal of Biomechanics, vol. 45, no. 6, pp. 1048–1052, 2012.

[5] S. Riek, A. E. Chapman, and T. Milner, “A simulation of muscle force and internal kinematics of extensor carpi radialis brevis during backhand tennis stroke: implications for injury,” Clinical Biomechanics, vol. 14, no. 7, pp. 477–483, 1999. [Online]. Available: https://www.sciencedirect.com/science/article/pii/S0268003398900973

[6] J. Christensen, J. Rasmussen, B. Halkon, and S. Koike, “The development of a methodology to determine the relationship in grip size and pressure to racket head speed in a tennis forehand stroke,” Procedia Engineering, vol. 147, pp. 787–792, 2016, the Engineering of SPORT 11. [Online]. Available: https://www.sciencedirect.com/science/article/pii/S1877705816307640

[7] K. Zhang, B. Guo, M. Yang, Y. Jia, K. Zhang, and L. Wang, “The assessment of sports performance by grip pressure using flexible piezoresistive pressure sensors in seven sports events,” Scientific Reports, vol. 14, no. 1, p. 31750, 2024.

[8] J. Rossi, E. Berton, L. Grélot, C. Barla, and L. Vigouroux, “Characterisation of forces exerted by the entire hand during the power grip: effect of the handle diameter,” Ergonomics, vol. 55, no. 6, pp. 682–692, 2012, pMID: 22458871. [Online]. Available: https://doi.org/10.1080/00140139.2011.652195

[9] T. L. Gibo, A. J. Bastian, and A. M. Okamura, “Grip force control during virtual object interaction: effect of force feedback, accuracy demands, and training,” IEEE transactions on haptics, vol. 7, no. 1, pp. 37–47, 2013.

[10] N. H. Kim, M. Wininger, and W. Craelius, “Training grip control with a fitts’ paradigm: a pilot study in chronic stroke,” Journal of Hand Therapy, vol. 23, no. 1, pp. 63–72, 2010.

[11] D. M. Wolpert, R. C. Miall, and M. Kawato, “Internal models in the cerebellum,” Trends in cognitive sciences, vol. 2, no. 9, pp. 338–347, 1998.

[12] R. Sigrist, G. Rauter, R. Riener, and P. Wolf, “Augmented visual, auditory, haptic, and multimodal feedback in motor learning: a review,” Psychonomic bulletin & review, vol. 20, no. 1, pp. 21–53, 2013.

[13] S. Furuya, T. Oku, H. Nishioka, and M. Hirano, “Surmounting the ceiling effect of motor expertise by novel sensory experience with a hand exoskeleton,” Science Robotics, vol. 10, no. 98, p. eadn3802, 2025.

[14] A. Topini, W. Sansom, N. Secciani, L. Bartalucci, A. Ridolfi, and B. Allotta, “Variable admittance control of a hand exoskeleton for virtual reality-based rehabilitation tasks,” Frontiers in neurorobotics, vol. 15, p. 789743, 2022.

[15] N. Ghobadi, W. Kinsner, T. Szturm, and N. Sepehri, “Embedded system for interactive pneumatic hand rehabilitation: Real-time gaming interface with cognitive stimulation for motor recovery,” IEEE Access, 2025.

[16] Y.-B. Liou, V.-T. Ngo, and Y.-C. Liu, “Designing a robot-assisted rehabilitation system for hand function recovery using virtual reality and haptic robot,” Advanced Robotics, vol. 38, no. 19-20, pp. 1392–1407, 2024.

[17] L. Yang, F. Zhang, J. Zhu, and Y. Fu, “A portable device for hand rehabilitation with force cognition: Design, interaction, and experiment,” IEEE Transactions on Cognitive and Developmental Systems, vol. 14, no. 2, pp. 599–607, 2021.

[18] Y. Chen, An evaluation of hand pressure distribution and forearm flexor muscle contribution for a power grasp on cylindrical handles. The University of Nebraska-Lincoln, 1991.

[19] K. FALCONER, “Quantitative assessment of cocontraction at the ankle joint in walking,” Electromyogr Clin Neurophysiol, vol. 25, pp. 135–148, 1985. [Online]. Available: https://cir.nii.ac.jp/crid/1572261549190540288